An Efficient Detail Preserving Diffusion Filter for Speckle Corrupted SAR Images

Aswathy S L
PG Scholar , Dept. of ECE
Muslim Association College of Engineering
Thiruvananthapuram , India

Sareena R
Asst. Professor, Dept. of ECE
Muslim Association College of Engineering
Thiruvananthapuram , India

Abstract— The hardest problem to be tackled in the field of Synthetic Aperture Radar (SAR) image processing is speckle. In the SAR imagery, multiplicative speckle noise generally reduces the performance of automatic scene segmentation and classification algorithms. To tackle such an issue, an anisotropic diffusion filter that manages to simultaneously fulfill competing requirements : reduce noise on homogeneous regions , preserve weak edges, and keeping corners and hard targets intact is proposed. Moreover since this efficient detail preserving diffusion filter is a partial difference equation based filter, no noise model was presupposed, so that in principle it can be applied to any noise type.

Index Terms—Anisotropic filters, image denoising, nonlinear filters, speckle, synthetic aperture radar (SAR) images.

I. INTRODUCTION

Many imaging technologies operate coherently to acquire images and as such are subject to speckling effects that greatly reduce observable details. For example, in synthetic aperture radar (SAR) imagery, speckle generally reduces the performance of automatic scene segmentation and classification algorithms. Presupposing the multiplicative speckle model, many despeckling filters have been designed to remove this kind of noise. Classic filters, such as Lee, Kuan, Frostand Gamma maximum a posteriori (MAP) [1], exploit the pixel values inside a small window centered at a given pixel to make inference and reconstruct its true value. In particular, in addition to multiplicative noise assumption, such filters presuppose the image to be as an ergodic process where statistical means can be substituted by spatial means. Even though these classic filters manage to reduce speckle on homogeneous areas, they completely fail to reconstruct the scene whenever an edge is in the local sliding window. In order to avoid such a behavior, a sharp transition inside the local window has to be treated in a different way. Nevertheless, edge detectors relying on a classical gradient operator produce signal-dependent results, and finer statistical edge detectors have to be used for this scope [1].

More recently, denoising filters based on the nonlocal means paradigm [3] have been designed to remove multiplicative speckle noise in SAR images [4]. In the design of the probabilistic patch based (PPB) filter in [4], Nakagami distribution of the SAR image amplitude is presupposed. Furthermore, a Bayesian framework is used to compute both a similarity measure among patches and the weighted mean used for pixel reconstruction. Due to its impressive visual results and since its performance outperforms even more sophisticated wavelet-based methods [5], PPB presents itself as a state-of-the-art reference for despeckling algorithms. Although effort has been dedicated to adapting the filters in [4] and [5] from the additive to the multiplicative noise model, denoising filters in [6] do not require this adaptation. In fact, contrarily to the afore-mentioned despeckling filters, these are nonlinear diffusion (NLD) filters that do not need any prior assumption, i.e., they can be directly applied to any type of noise-corrupted image. In addition, since the final result is a solution of a partial differential equation (PDE), many theorems and properties hold for such a solution (e.g., invariance to gray level shift, invariance to reverse contrast, invariance to image translation and rotation, preservation of average gray level, it respects the maximum-minimum principle, etc.) [7]. Nevertheless, even though several contributions and improvements (see [8]–[11]) have been made, little is known about the use of such filters for speckle removal. Furthermore, none of the filters described so far considers the edge and target preservation as a primary goal.

In this paper, a novel NLD denoising filter aimed at edge and target preservation is devised. Moreover, to validate this approach, a comparison with other state-of-art despeckling filters has been performed on a real 1-look CSK image.

II. NLD FILTERS

A. Theoretical Background

Some very powerful classes of despeckling filters are those that compute the solution of a PDE applied to the image. As an example, filtering an image with a Gaussian kernel G_σ , where σ indicates the Gaussian standard deviation, it is equivalent to considering each gray level in the original image as a temperature measurement. Formally, each value of the gray level image I, $I \subset \mathbf{R}^2 \rightarrow \mathbf{R}$, is considered a physical variable such as temperature so that the existence of the concentration gradient ∇I creates a flux $J = D \cdot \nabla I$ to equilibrate the concentration differences in the diffusing medium (Fick's first law), with D the diffusion tensor (a 2×2 matrix) that characterizes diffusing medium. Since the mass conservation hypothesis has to be respected, the temporal variation of I inside medium is equal to the flux J across the

boundary of medium (Fick's second law)

$$\frac{dI}{dt} = div(D \cdot \nabla I) \quad (1)$$

with *div* the divergence operator. In fact, in principle, the application of an NLD filter is equivalent to solving the PDE in (1) superimposing the noisy image as the initial condition at time $t = 0$. where I_0 is the initial noisy image.

B. Related Works

Clearly, without any modification to (1), the natural evolution of the system leads to a completely blurred image. To solve this problem, Oliver and Quegan [1] propose the matrix D with a scalar function $g(\nabla I)$ that is reversely proportional to the image gradient module. It should be noted that inverse proportionality between $g(\nabla I)$ and $|\nabla I|$ enables the filter to stop diffusion (smoothing) on edges (i.e., points with high value of $|\nabla I|$). The Perona–Malik (PM) article [1] has been the basis of many proposed evolutions, and an interested reader can find a detailed overview in [10]. Nevertheless, even though these filters are often referred to as anisotropic diffusion techniques, the first real anisotropic diffusion approach was proposed in [7], where the coherence enhancing diffusion (CED) was devised. Practically speaking, in CED, the diffusion matrix D is not substituted by a scalar function; instead, its elements are etrieved from the image structure tensor $S(\nabla I\sigma)$. Once $S(\nabla I\sigma)$ is smoothed element-wise by $G\rho$ to reduce the noise, the resultant matrix $S\rho$ (symmetric and positive semi-definite) can be decomposed to find the image principal components. The diffusion matrix can be derived as:

$$D = [v_1\ v_2] \begin{bmatrix} g_{\lambda 1}(\lambda_1, \lambda_2) & 0 \\ 0 & g_{\lambda 2}(\lambda_1, \lambda_2) \end{bmatrix} \quad (2)$$

with $g_{\lambda 1}(\lambda_1, \lambda_2) = \alpha$ and

$$g_{\lambda 2}(\lambda_1, \lambda_2) = \alpha + (1 - \alpha) e^{\frac{-C_m}{(k/(\lambda_1 - \lambda_2)^2)^m}} \quad (3)$$

where α permits a small diffusivity (usually $\alpha = 0.05$) even when no preferential direction exists and k acts as a threshold to $(\lambda_1 - \lambda_2)^2$ value. Moreover, the positive constant Cm is introduced to correct the bias in the original Perona–Malik diffusivity function [7]. Since the aim of [7] was not to devise a denoise filter, applying CED on a speckle-corrupted image yields results with completely distorted details. However, as suggested in [10], an edge enhancing diffusion requires modifications to diffusivity functions according to following relation :

$$|\nabla I| \to \infty, \quad g_{\lambda 1}(\lambda_1, \lambda_2) / g_{\lambda 2}(\lambda_1, \lambda_2) = 0. \quad (4)$$

III. Detail Preserving Diffusion (DPD) Filter

We propose the following modifications to the CED schema to keep the real anisotropic behavior of CED while respecting the relation in (5)

$$\begin{cases} 1 - e^{\frac{-C_{m1}}{(k_1/\lambda_1)^m}} \\ 1 - e^{\frac{-C_{m2}}{(k_2/\lambda_2)^m}} \end{cases} \quad (5)$$

The choice in (6) can be better appreciated exploiting a convenient decomposition of the flux J. With indicating the eigen values of diffusion matrix D as $\mu 1 = g_{\lambda 1}(\lambda_1)$, $\mu 2 = g_{\lambda 2}(\lambda_2)$ and the image derivatives along v_1, v_2, respectively, with I_{v1} and I_{v2}, the flux J can be decomposed as:

$$J = \mu 1 I_{v1}\, v_1 + \mu 2 I_{v2}\, v_2 \quad (6)$$

Therefore, using the diffusivities in (6), three different filter behaviors are highlighted by the novel IEED filter.

1) On homogeneous *areas* both $\lambda 1$ and $\lambda 2$ are low. Therefore, $\mu 1$ and $\mu 2$ are near 1, i.e., an isotropic diffusion case (speckle removal).
2) On edges λ_1 is high and λ_2 is low. Consequently, $\mu 1$ is near **0** and $\mu 2$ is near 1, i.e., an anisotropic diffusion case with smoothing along v_2 (edge preservation).
3) On corners both λ_1 and λ_2 are high. As a consequence, μ_1 and μ_2 are near **0**, i.e., a no diffusion case (corner preservation).

It should be noted that the last behavior avoids shape distortion of objects and hard targets smoothing. In fact, not only corners and singularities, but also small objects with high radar cross section (RCS), are characterized by a high value of both λ_1 and λ_2, thus causing diffusion stop. Summarizing, with the diffusivity in (2), we manage to effectively combine the respective advantages of the PM and CED filter. In the PM schema, the speckle on homogeneous regions is removed but there is no diffusion along edges, so they remain noisy in the final result. Conversely, the CED filter provides little speckle removal on homogeneous areas, but edges are correctly reconstructed.

A. Algorithm Description

Usually, the edge detection problem in noisy images is tackled by directly or indirectly using information related to the image gradient. Nevertheless, in the SAR community, the image coefficient of variation C_I is more commonly used to face the same issue in despeckling filter implementation [8]. Even though the multiplicative speckle assumption justifies this choice [2], a simple logarithmic transformation solves the previous problem, allowing a gradient operator to be used for edge detection in SAR images. As an example, the SRAD filter in [8] and its anisotropic extension in [11] use C_I to avoid biased gradient operations. However, they both use numerical implementation where differences between near values are computed, thus nullifying the advantages. For these reasons, in our filter implementation, a logarithmic transformation is applied to the input image, and a reverse exponential function is operated to the end. Furthermore, the structure tensor matrix in (4), which relies on the gradient information, is utilized as an edge detector.

With regards to unknown variables, both diffusivities in (8) depend on two parameters, namely, the threshold k_i and the exponent m_i, with i = 1, 2. In order to have the same behavior in both directions, the exponent m_i has been set equal for both diffusivities ($m_1 = m_2 = m$), and a value of m = 16 has been selected to have a fast transition of the diffusivity function from **0** to **1** around the threshold k. Instead, exploiting a homogeneous area of the processing image, each threshold k_i

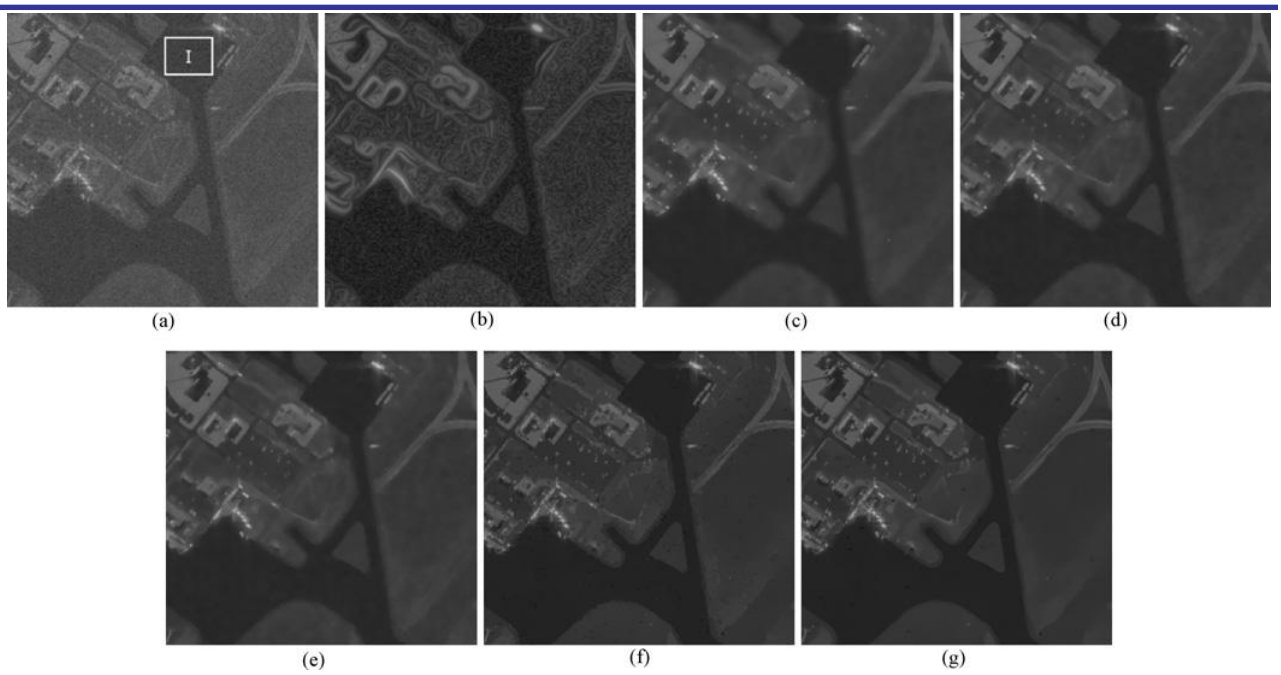

Fig. 1. Despeckling results on a CSK image acquired over Tucson, AZ—Courtesy of Agenzia Spaziale Italiana (ASI). (a) Original. (b) CED. (c) SRAD.(d) PPB. (e) Iterative PPB. (f) PM. (g) DPD

is estimated by the corresponding quantile Q_i—set by the user as an input parameter—of the experimental cumulative density function (ecdf) of the respective eigenvalue λ_i. In this way, the thresholds k_i are automatically adjusted at each step by the degree of despeckling reached at that point. It should be noted that to avoid user selection of a homogeneous area, the C_I index of the original noisy image can be com-puted and thresholded to yield a binary mask. In this way, only the pixels belonging to this mask are used in the ecdf computation.

Another improvement of the detail preserving diffusion filter performance with respect to the filters presented in [1]–[9] and [11] is the use of an appropriate numerical schema [12] to compute the solution of the PDE . In fact, the schema was optimized for rotational in variance, which is a fundamental property when the gradient computed along the main axes is used for di-rectional derivatives. Moreover, the explicit numerical schema proposed in [12] combines the advantages of classical (Euler forward) explicit schemas of yielding a small error in final solution computation, with a higher efficiency (up to four times) typical of implicit or semi-implicit techniques. Indeed, a time step up to t = 1 can be used without compromising the numerical stability. Finally, the numerical computation in [12] can be directly implemented by simple convolution operations. In fact, in [12], all derivatives are computed by means of a simple Sobel-like 3 × 3 derivative mask at the place of the classical stencil-like schemas [10].

IV. EXPERIMENTAL RESULTS AND ANALYSIS

This section describes the despeckling experiments per-formed on an actual SAR image [see Fig. 1(a)] to illustrate the effectiveness of the proposed method. The DPD filter was compared to NLD filters such as PM [1] and SRAD [8]. Furthermore, the promising PPB filter [4] (with and without iterations) was considered state-of-the-art reference. The SRAD filter was implemented with the classical Euler-forward schema. Moreover, a time step $t = 0.5$ and $n = 200$ iterations were selected to obtain stable results. Finally, a homogeneous region of the image was passed as input to enable the filter to compute the instantaneous coefficient of variation [8]. The same homogeneous region was also passed in input to PM and DPD to estimate the respective thresholds. PM was implemented with the same numerical schema as DPD and the threshold k was estimated by the quantile $Q = 0.95$ of the gradient module ecdf. For the DPD filter, the edge-controlling quantile was set to $Q_1 = 0.95$ and the corner-controlling quantile was set to $Q_2 = 1$. Note that having the ecdf computed on a homogeneous area, the value $1-Qi$ is an estimate of the false alarm probability of the respective edge ($i = 1$) and corner ($i = 1$) on it. In fact, the previous values of Q_1 indicate that on a noisy homogeneous area, 5% of the λ_1 occurrences have values comparable to the ones obtained on edges. The same applies for corners where Q_2 has been set to 1, presupposing no corners or singularities within the homogeneous region in input. Therefore, the quantile Q_2 may be lowered for a stronger corner (target) preservation and the quantile Q_1 can be raised if only strong edges are concerned. Moreover, a Gaussian kernel with standard deviation σ_1 was applied before filtering (in order to make the initial image differentiable), and we selected $\sigma_1 = 0.5$ to minimize the loss in resolution. Then, at each step, a Gaussian kernel with $\sigma_2 = 1$ was applied as regularization [9].

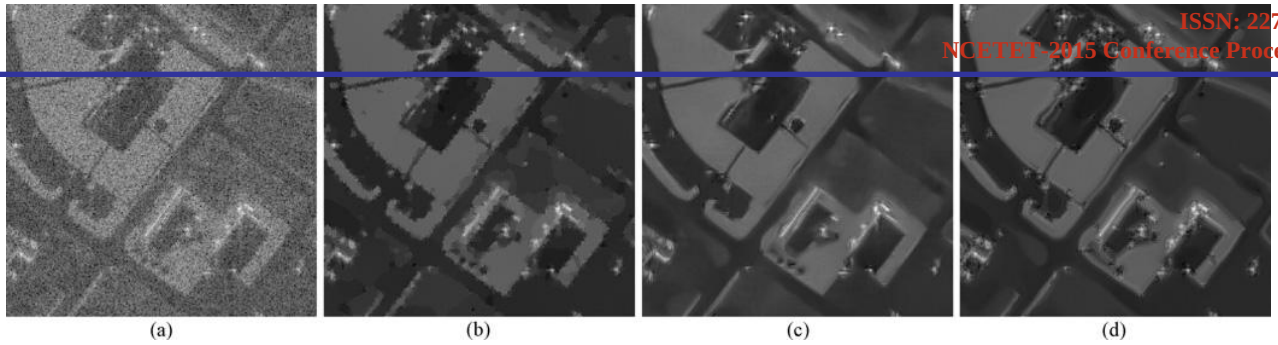

Fig. 2. Despeckling results on a heterogeneous area with buildings. (a) Original. (b) PM. (c) Iterative PPB. (d) DPD.

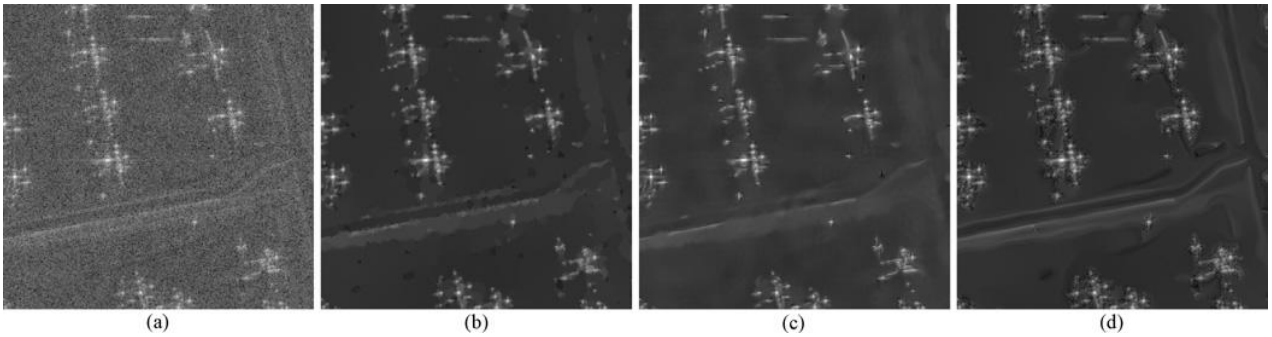

Fig. 3 . Despeckling results on an area with hard targets and small roads. (a) Original. (b) PM. (c) Iterative PPB. (d) DPD.

The non iterative PPB filter parameters were set according to author suggestions [4], i.e., number of looks $L = 1$, search windows 21×21, similarity window 7×7, h-parameter quantile $\alpha = 0.88$. The same applies for the iterative PPB filter, where the variable window size optimization was used [4] with $\alpha = 0.92$, $T = 0.2$, and 25 iterations. The results of the evaluated despeckling algorithms are shown in Fig. 2 for a CSK image acquired over Tucson, AZ, USA, with the following characteristics: product L1A, Spotlight 2 acquisition mode, polarization HH, incidence angle 24°, and number of looks $L = 1$. The images are 16-bit deep and they are shown after a logarithmic transformation $l_2 = \log_2(l + 1)$.

Then, the same linear mapping of dynamic range between **0** and $2^{16} - 1$ was applied to each result to further improve visualization and comparison. It should be pointed out that the result yielded by CED is reported only for the sake of visual comparison, since CED does not deal with noise removal but it aims to complete interrupted lines and enhance flow-like structures (e.g., enhancement of fingerprint images). As can be seen from the results, application of the SRAD filter loses even some large details. Moreover, targets are distorted and observed as bright blobs. The PM filter reveals small RCS variations, however, the region boundaries remain noisy. The PPB filter introduces some artificial texture on homogeneous areas and some edges and targets are blurred. Instead, the iterative PPB filter retrieves target sharpness, but some edges and fine details are not retrieved by iterations. Furthermore, the PPB filter increases the dynamic range at each iteration, i.e., low values are lowered and high values are increased.

Clearly, this behavior tends to generate some artifacts, such as dark spots besides brighter areas. Differently, the DPD filter preserves even small details and weak edges. In addition, the dynamic range extension is theoretically avoided since the maximum–minimum principle has to be respected by the PDE solution. The considerations can be further appreciated for PM ,iterative PPB, and detail preserving diffusion filters by the magnifications in Figs. 2 and 3. As can be clearly seen from these figures, only the diffusion filter manages to fully remove speckle without smoothing the finest details.

V. CONCLUSION

In this paper, we presented a new anisotropic diffusion filter that managed to combine normally contrasting requirements: reducing noise on homogeneous regions, preserving weak edges, and keeping corners and targets intact (maintaining them as seen in the original image). Moreover, since DPD filter is a PDE-based filter, no noise model was presupposed so that, in principle, it can be applied to any noise type. This last property had a strong impact on its possible application. In fact, no mathematical modeling effort was required (e.g., statistical modeling of both noise and radar reflectivity) to change sensor or data type (e.g., intensity or amplitude). In addition, since the filtered image was a solution of a PDE, many theorems and properties hold for such a solution. Finally, visual impressions and performance indexes confirmed that DPD filter outperformed state-of-the-art filters for SAR image despeckling.

ACKNOWLEDGMENT

We would like to express our sincere gratitude and heartful indebtedness to all Professors, Department of Electronics and Communication Engineering, MACE for their help and support. Also we are grateful to Dr. S Ibrahim Sadhar who helped in getting SAR images and for his valuable suggestions.

REFERENCES

[1] C. J. Oliver and S. Quegan, *Understanding Synthetic Aperture Images*. Norwood, MA, USA: Artech House, 1998.

[2] R. Touzi, A. Lopes, and P. Bousquet, "A statistical and geometrical edge detector for SAR images," *IEEE Trans. Geosci. Remote Sens.*, vol. 26, no. 6, pp. 764–773, Nov. 1988.

[3] A. Buades, B. Coll, and J. M. Morel, "Image denoising methods. A new
Non local principle," *Siam Rev.*, vol. 52, no. 1, pp. 113–147, Jan. 2010.

[4] C.-A. Deledalle, L. Denis, and F. Tupin, "Iterative weighted max-imum likelihood denoising with probabilistic patch-based weights," *IEEE Trans. Image Process.*, vol. 18, no. 12, pp. 2661–2672, Dec. 2009.

[5] H.-C. Li, W. Hong, Y.-R. Wu, and P.-Z. Fan, "Bayesian wavelet shrink-age with heterogeneity-adaptive threshold for SAR image despeckling based on generalized gamma distribution," *IEEE Trans. Geosci. Remote Sens.*, vol. 51, no. 4, pp. 2388–2402, Apr. 2013.

[6] P. Perona and J. Malik, "Scale-space and edge detection using anisotropic diffusion," *IEEE Trans. Pattern Anal. Mach. Intell.*, vol. 12, no. 7, pp. 629–639, Jul. 1990.

[7] J. Weickert, "Coherence-enhancing diffusion filtering," *Int. J. Comput. Vision*, vol. 31, nos. 2–3, pp. 111–127, 1999.

[8] Y. Yu and S. Acton, "Speckle reducing anisotropic diffusion," *IEEE Trans. Image Process.*, vol. 11, no. 11, pp. 1260–1270, Nov. 2002.

[9] F. Catté, P. Lions, J. Morel, and T. Coll, "Image selective smoothing and edge detection by nonlinear diffusion," *SIAM J. Numer. Anal.*, vol. 29, no. 1, pp. 182–193, 1992.

[10] J. Weickert, *Anisotropic Diffusion in Image Processing* (ECMI). Stuttgart, Germany: Teubner, 1998.

[11] K. Krissian, C. Westin, R. Kikinis, and K. Vosburgh, "Oriented speckle reducing anisotropic diffusion," *IEEE Trans. Image Process.*, vol. 16, no. 5, pp. 1412–1424, May 2007.

[12] J. Weickert and H. Scharr, "A Scheme for coherence-enhancing diffusion filtering with optimized rotation invariance," *J. Visual Commun. Image Represent.*, vol. 13, nos. 1–2, pp. 103–118, 2002.

.

.